SEVERE ACCIDENT ANALYSIS CODE SAMPSON FOR IMPACT PROJECT

HIROSHI UJITA, TAKASHI IKEDA, AND MASANORI NAITOH

Address: Advanced Simulation Systems Department, Nuclear Power Engineering Corporation
Fujita Kanko Toranomon Bldg., 6F, 17-1, 3-chome Toranomon, Minato-ku, Tokyo, 105-0001 JAPAN

E-mail : ujita@nupec.or.jp, t-ikeda@nupec.or.jp, ms-naitoh@nupec.or.jp

Key Words: Severe - Thermal - Hydraulics

Four years of the IMPACT project Phase 1 (1994-1997) had been completed with financial sponsorship from the Japanese government's Ministry of Economy, Trade and Industry. At the end of the phase, demonstration simulations by combinations of up to 11 analysis modules developed for severe accident analysis in the SAMPSON Code were performed and physical models in the code were verified. The SAMPSON prototype was validated by TMI-2 and Phebus-FP test analyses. Many of empirical correlation and conventional models have been replaced by mechanistic models during Phase 2 (1998-2000). New models for Accident Management evaluation have been also developed.

Introduction

IMPACT, 'Integrated Modular Plant Analysis and Computing Technology', is the name of a program and of specific simulation software, which will perform full-scope and detailed calculations of various phenomena in a nuclear power plant for a wide range of event scenarios [1-6]. The main analysis objectives are to show that light water reactors (PWR/BWR) maintain adequate safety margin under hypothetical severe accident conditions and to investigate realistic measures of accident management by simulating the accident in detail and on a reasonable time frame using a parallel computer. To satisfy the objectives, physical and chemical phenomena during fuel cladding damage, fuel melting, candling, crust forming, molten debris cooling, fission products release and transport, debris-concrete interaction, steam explosion, hydrogen mixing and burning, etc., must be calculated and reactor vessel and containment structural integrities must be evaluated. Because it is difficult to clarify various phenomena in the full-range of an accident scenario by experiments that pinpoint the significant events and investigate the specific phenomena in detail, analysis must be relied upon for understanding the entire scope of a severe accident. Evaluation of safety margin and accident management procedures requires mechanistic models describing the phenomena in detail and accurate computing methods. To satisfy these analytical needs, computer simulations must be based upon fundamental physics principles and sophisticated modeling. Calculation of the full scope of a severe accident using mechanistic models requires a

large computational time, therefore, codes in IMPACT are being developed in a parallel environment. Separate software modules for micro-, meso-, and macro-scale modeling are being developed which may be combined in the most systematically efficient manner, for easy modification and maintenance of the codes.
At the end of Phase1 (1994-1997), the verification study of SAMPSON prototype was conducted in two steps. First, each analysis module was run independently and analysis results were compared and verified against separate-effect test data with good results. Second, up to 11 analysis modules were executed concurrently in the parallel environment, to demonstrate the code capability and integrity by analyzing Surry LOCA scenario [7-11].
SAMPSON prototype was further validated by TMI-2 accident and Phebus-FPT0 test analyses in 1998.
In Phase2 (1998-2000), as for the models using for In-Vessel Retention analysis, mechanistic models were improved as follows: multi-dimension in in-vessel analysis modules; fuel cladding failure by melt, embrittlement, or ballooning; diversity in phase change and interfacial convection during molten core relocation; gap cooling and CCFL models for debris cooling; grain growth & movement and uranium oxidization during FP release; pool scrubbing and re-evaporation models in FP behavior; etc. As for the Accident Management evaluation, following models were developed: RPV external cooling of debris; hydrogen mixing and deflagration; PCV venting; ESF effects models; etc.
Code will be enhanced by application use in Phase3 (2001-2002).

In the present paper, typical model improvement and verification process in Phase 2 will be presented. Phebus test analysis, phase change and fluid dynamics models improvement and verification in molten core relocation analysis module, debris cooling model and water ingression into gap model improvement and verification in debris coolability analysis module, and FP release from fuel pellet model improvement and verification are described.

Phebus/FPT0 Experiment Analysis

Phebus FP is the ongoing program to investigate, through a series of integral in-pile experiments, key-phenomena involved in the progression of a postulated severe accident in a light water reactor. The FPT0 test [12] performed at the Cadarache Nuclear Research Center as the first test of planned six in-pile tests. The bundle consists of 1 m long 20 fuel rods of typical PWR geometry, assembled with two Zircaloy spacer grids. At the center of the bundle, there is a silver-Indium-cadmium control rod with a stainless steel cladding and a Zircaloy tube.

The fluid dynamics of the Phase-1 MCRA (molten core relocation analysis module) is one dimensional in vertical direction, but the module can treat heat transfer between channels with heat structure model. Two channels are set up, one is for fuel bundle and another is for shroud cooling channel. The identical 20 fuel rods are set in the inner channel. The shroud is composed of 4 oxidized metal and one Inconel layers. Zircaloy material properties are used for inner 4 layers and steel material properties, for the outer layer since detailed material properties were not available. The shroud is modeled with

Slab heat structure. The control rod was not involved in the calculation since its model of FRHA (fuel-rod hear-up analysis module) was obviously incapable of accounting the control rod failure effect on the fuel failure process. The module did not model the control rod mechanistically but only considered its heat capacity in the hase-II development scope.
Axial calculation cells for MCRA from k=2 to k=12 are assigned to FRHA, where k=2 of FRHA is a structure cell so from k=3 to k=12 corresponds a fuel column. The blockage and obstacle models are used. Spacers are set at k=4 and 8 in vertical direction resulting large friction at the upper surface of these two cells. Hence, liquid fuel and fuel particle are to be stored in cell k=5 and 9. Preliminary calculation for the 1st (0-3445 s), 2nd (-6485 s), and 3rd (-10140 s) phases was done to obtain the fuel rod temperature distribution at the transient inception with FRHA and a simple thermal hydraulics model attached to FRHA. The calculated maximum temperatures of a fuel rod in 2nd and 3rd phases were 846 K and 1085 K, respectively, which showed reasonable agreement with those of about 873 K and 1173 K in the experiment.

Calculation was started with FRHA and MCRA at 10,000 s of the experiment and expressed it as 0 s. The outlet cladding temperature is not always the maximum because the first channel is cooled due to the heat transfer through shroud. The steep temperature rise shows the cladding failure at the axial cell.
The fuel rod fails at k6 at about 2,300 s, then at k7, k8, k5, and k9 in sequence. Liquid fuel decreases after release because it freezes into solid particle component or onto cladding and shroud surfaces as crust.
Fuel particle component is accumulated in k5, k9, and k6 cells due to the obstacle model. It is also due to freezing of liquid zircaloy component that it decreases after release into the channel.
The time of fuel failure initiation in the calculation is a little earlier than the experimental knowledge. At the time 4,500 s, the fuel bundle remains intact under the lower spacer in calculation and experiment, but the fuel bundle between spacers disappears in calculation while a part of it remains in the experiment, that is, the calculated physical phenomena seems to develop faster than the experiment. Furthermore, a part of the fuel is liquefied after failure due to eutectics in experience while there is little fraction of fuel is in liquid in calculation. The disagreement between experiment and calculation is caused mainly by the following items:
(a) Inappropriate fuel failure criterion in FRHA, that is, a lack of liquefaction mechanism of control and fuel material,
(b) Absence of radiation model from fuel bundle to shroud, and
(c) Limitation of one-dimensional calculation in MCRA that makes it impossible to take the radial power distribution and the steam flow redistribution in the inner channel into consideration.

Figure 1 shows bar graphs of the volume fractions of components in every axial cell at the time 8,000 s.

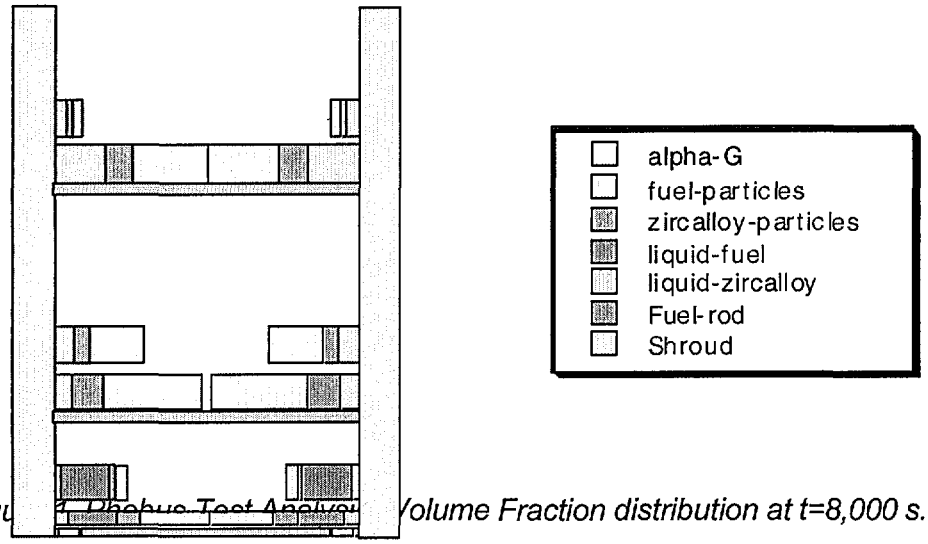

Figu[illegible] Volume Fraction distribution at t=8,000 s.

2D Fluid Dynamics and Phase Change Model

MCRA has been multi-dimensionalized, while two-dimension R-Z co-ordinates calculation function will be used for core region. Two types of dam break problems with X-Z and R-Z co-ordinates are calculated and compared with experimental data with good agreement.

Phase transition paths such as melting/ solidification in fuel, zircaloy and steal particles, and of interaction between fuel liquid and fuel particle, evaporation/ condensation paths between water and high temperature liquid or particle, etc. are added. 7 types of paths were tested with satisfactorily.

To verify these improvement, the system, which simulates molten fuel relocation to lower plenum appeared in TMI2 accident, shown in Figure 2(a) is used. Buffle plate melted by molten fuel and melt fallen down from the side wall to lower plenum, where fuel interact with the water in the bottom. The repetition of plug and falling of melt was observed in Figure 2(b).

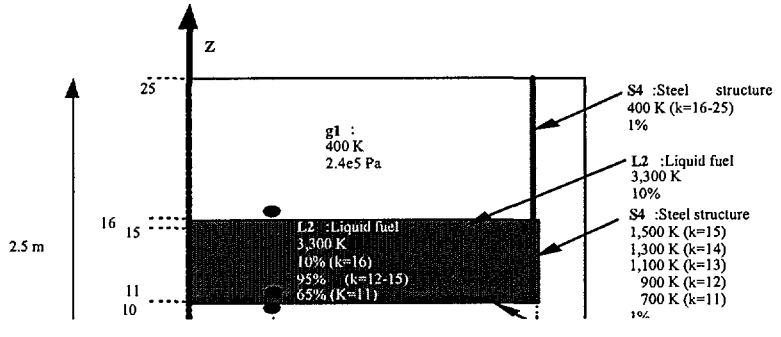

(a) System analyzed

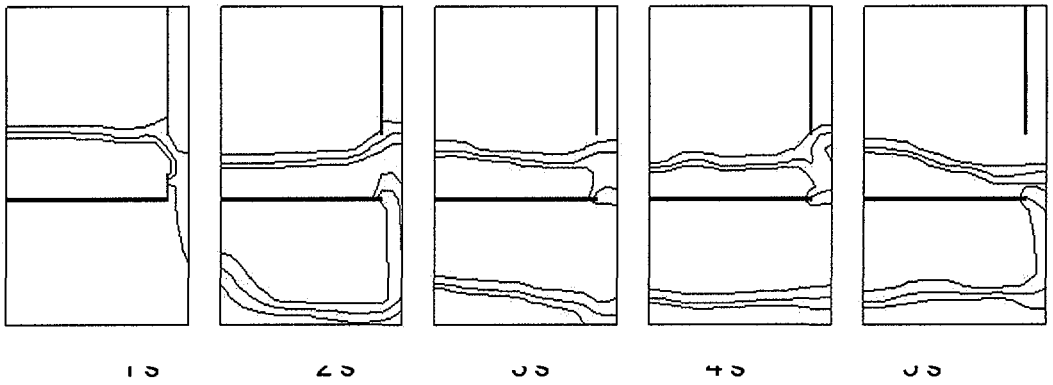

(b) Volume Fraction of Molten Fuel

Figure 2. Verification of phase change & 2D fluid dynamics.

Debris Cooling Model

For the three-dimensional debris cooling model, the verification was performed by focusing on the capability for simulating the three-dimensional natural convection.

Toda et al. [13] have carried out a natural convection experiment using atmospheric water as a working fluid. The test section was an acrylic cylindrical enclosure of 0.1m height and 0.094m inner diameter as shown in Figure3. The copper cooling plate was arranged above the test section and kept at constant temperature by a cooling water flow inside the plate. The walls of the ide and bottom were adiabatic. Sixteen thermocouples were installed in the test section for measurement of the temperature distribution. The temperature difference from the cooling surface was measured vertically at four horizontal positions. Internal heating was supplied by electrical joule heating from a coil nichrome wire of 10mm diameter and 9mm length. The coil was arranged eccentrically in the test section. The heating rate was set at 5.25 W or 14.6 W.

The temperature above the internal heat source increased, however, the temperature below it remained low due to stagnation in the experiment. The temperature was

measured after the flow was considered to reach the steady state and the experimental results were compared with calculation results made for steady state conditions. Comparison showed that their analytical results differed a little from the experimental ones, especially for high heating rate. It seemed that the heat loss from the test section influenced the convection and a heat loss evaluation was required in the analysis. The copper cooling plate was arranged as a solid mesh and the analysis of heat conductivity inside the cooling plate and natural convection in water were performed as a continuum due to the ability of the debris cooling model. The uniform temperature of a fluid and cooling surface was given as the initial condition. The steady state condition of the analysis was judged when the flow was fully developed and the velocity fluctuation at every mesh became within 0.1% for a calculation step. 3.0 10^5 steps were needed to obtain the steady state condition in this verification analysis.

The results showed a hot region right above the internal heat source and a cold stagnant region below it. Large convection cells of an ascending flow from the internal heat source and a descending flow along with the side wall were formed, and lower velocity vectors were evident in the stagnant region of the vessel lower part. The temperature and velocity vector distributions erewcon sided to be qualitatively appropriate. Comparisons between the calculated vertical temperature difference from the cooling surface at four horizontal positions and the experimental data when the flow was fully developed are shown in Fig.4 (b). The horizontal axis shows the vertical distance from the cooling surface and the vertical axis shows the temperature difference between the fluid temperature and the cooling surface temperature. The maximum fluid temperature at each heating rate was well simulated and the calculated temperature profile along the distance from the cooling surface was considered to reproduce the experimental data. Though there was a temperature difference of 1.0K between the upper value in the experiment and the calculation at the lower part of the MR-line, this difference was considered to be caused by the heat loss at the side wall. The necessity of the heat loss evaluation was also pointed out by Toda, et al. The results showed the capability of the debris cooling model for obtaining the fluid temperature distribution of three-dimensional natural convection.

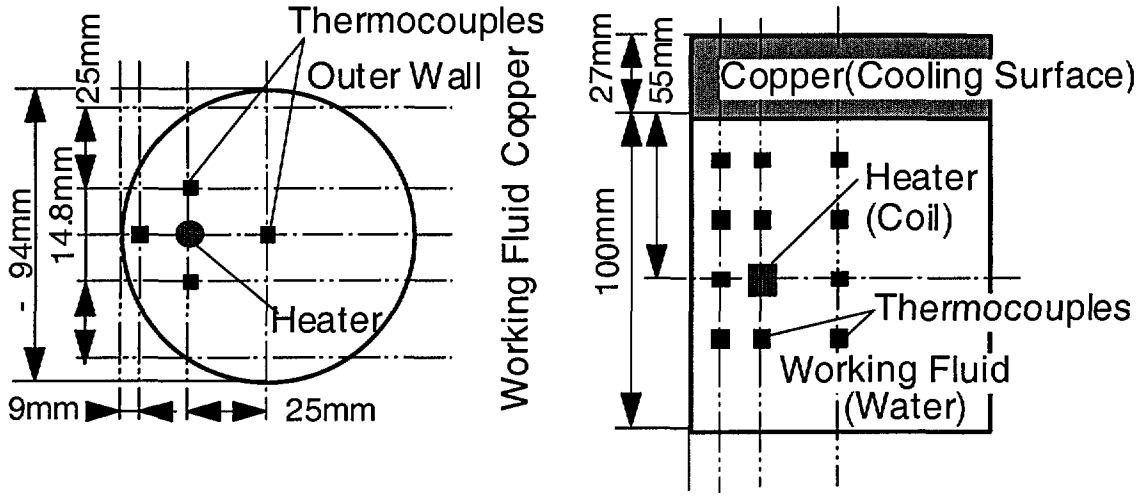

(a) Experimental Apparatus

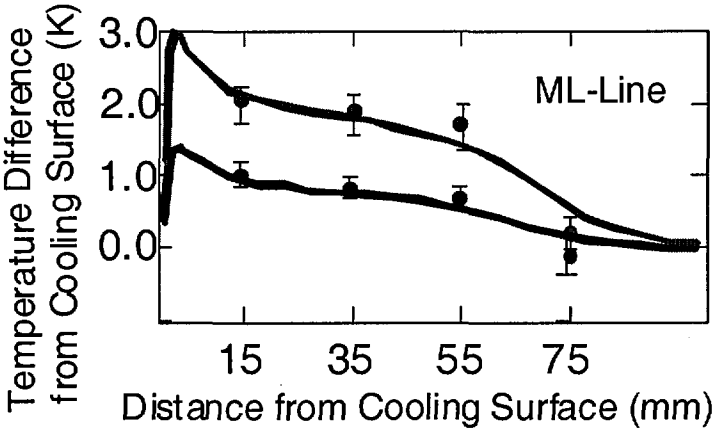

(b) Comparison between Calculation and Experiment

Figure 3. Experiment by Toda et al.

Water Ingression into Gap Model

The water ingression at the gap entrance was evaluated based on the heat and mass balance as proposed by Fujita and Uchida [14]. The water ingression velocity was calculated by the CCFL Wallis correlation, where a dimensionless superficial velocity of steam is determined from the steam generation rate in the gap. The water ingression length is related to the water mass by the void fraction as the gap volume-length function. The void fraction was calculated based on the drift-flux model.

Calculations were performed to alidate water ingression into the gap model. The boundary conditions were the same as the validation calculation of the debris cooling model, except for the debris-to-vessel gap width and primary system pressure. The gap widths were 1mm and 5mm at primary system pressures 0.1 MPa and 11.5 MPa. The single-phase option in the gap was selected for the preliminary analysis. Trends for the RPV wall temperature and the water ingression length are shown in Figure 4.
The water ingression length increased with the pressure decrease and the gap width, the RPV failure did not occur in the case that water reached the debris bottom. For high system pressure, water did not ingress into the gap even for the 5mm gap because the steam velocity increased for the effect of property.
The effects of the gap width and primary system pressure on the RPV wall heat load were relatively large. The evaluation of the water ingression behaviour was considered to be an important factor for the RPV safety margin. Parametrical studies are needed to clarify the characteristics of the gap cooling effect.

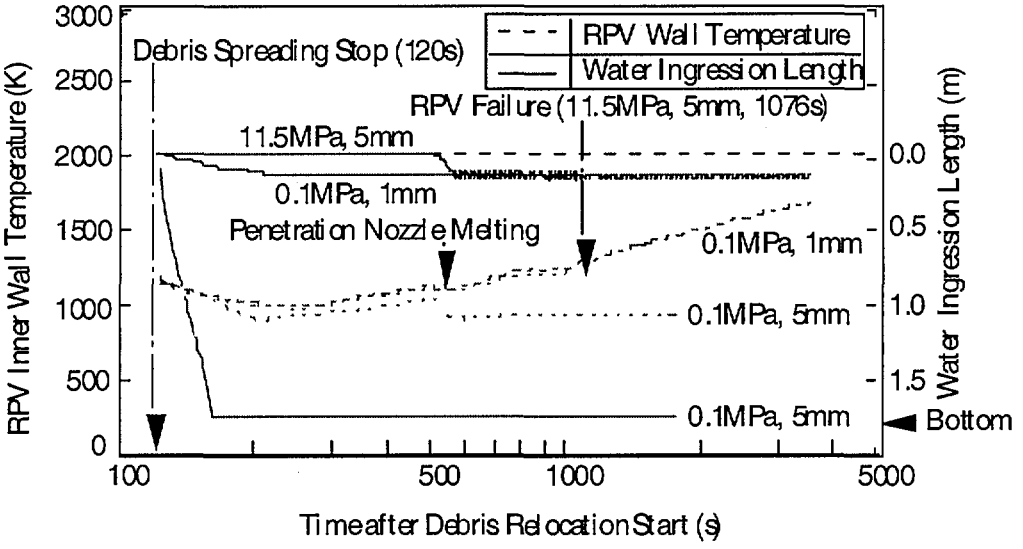

Figure 4. Water ingression trend into gap.

Release Model from Fuel Pellet

The basic equation is a three-dimensional mass balance equation for each fission product. In the pellet, diffusion and transfer due to the temperature gradient to the grain boundary are considered. A cylindrical grain is assumed in each mesh of the pellet. Fission products are accumulated at the grain boundary and assumed to be released to the gap when the concentration exceeds the certain value. As the volume of the grain increases with temperature, fission products are swept by the moving grain boundary. The amount of swept fission products is assumed to be proportional to the moving velocity of the grain boundary. The diffusion equation is solved by Euler's explicit method.

Diffusion coefficients for fission products are obtained based on release data [15]. The coefficients for fission products with low volatility are low due to the formation of oxides or uranates as follows [16],

$2Ba + O_2 = 2BaO$, $Ba + U + 2O_2 = BaUO_4$

$BaO + UO_2 + 1/2O_2 = BaUO_4$, $2Sr + O_2 = 2SrO$

In this model, the diffusion coefficients for fission atoms in the pellets are assumed to be the same as those for noble gases. The vapor of the oxide and uranates is assumed to be released directly from the pellets. So the amount of released fission products is the sum of diffusion and evaporation.

The partitionings were calculated using free energies of each species. Barium uranate ($BaUO_4$) is a stable compound at lower temperatures. Barium atoms, which are subject to diffusion, increase with the pellet temperature. Volatile barium oxide (BaO) also increases with the pellet temperature. In this module, the diffusion of barium atoms is solved and the vapor pressure of barium oxide is calculated based on the partitioning of barium species.

Calculated amounts of released krypton and barium were compared with the results of the ORNL VI-3 experiment. The fuel specimen was heated by RF power under steam atmosphere and the released fission products were measured using radiation detectors in the VI-3 experiment, while the fuel was 44 MWd/kgU. The fuel specimen was assumed to be a cylindrical grain with different x/z ratios, but the volume was equal to the spherical grain with a diameter of 12 m. The cylindrical grain was divided into 10 along the x-axis, 4 along the y-axis and 7 along the z-axis.

Figure 5 shows the release ratio of krypton as a function of time. Although there is little difference among cases with different x/z ratios, the case of x/z=2 is most comparable with the experimental results. This is reasonable because the fuel specimen is easily expanded toward the x direction. The amount of released krypton was increased by about a factor of 5 due to grain boundary sweeping.

The release ratio of barium atoms by diffusion in the pellets is calculated to be about 0.3 based on the partitioning of barium species. The release ratio of barium oxide is evaluated as 0.1. The total release ratio of barium is about 0.4, which is comparable with the measured ratio of 0.3.

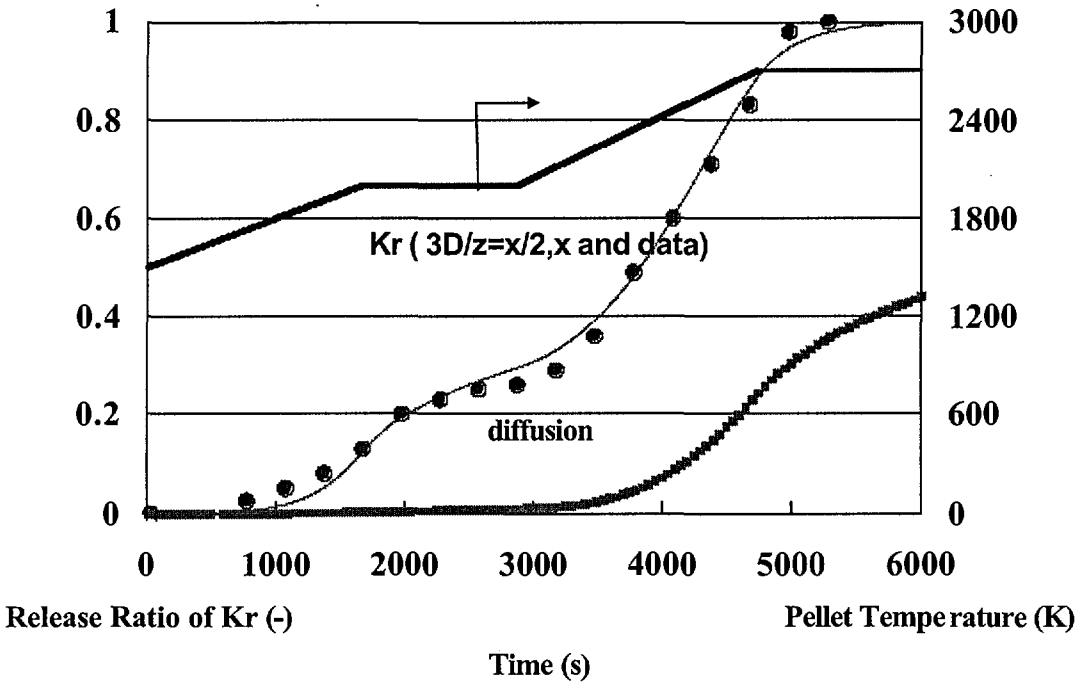

Figure 5. Release ratio of krypton as a function of time.

Conclusions

The IMPACT project Phase 1 (1994-1997) had been completed, and now Severe Accident Analysis Code SAMPSON has been improved in Phase2 (1998-2000).

At the end of Phase1, the verification study of SAMPSON prototype was conducted in two steps. First, each analysis module was run independently and analysis results were compared and verified against separate-effect test data with good results. Second, up to 11 analysis modules were executed concurrently in the parallel environment, to demonstrate the code capability and integrity by analysing Surry LOCA scenario.

SAMPSON prototype was further validated by TMI-2 accident and Phebus-FPT0 test analyses in 1998.

In Phase2, as for the models using for In-Vessel Retention analysis, mechanistic models were improved as follows: multi-dimension in in-vessel analysis modules; fuel cladding failure by melt, embrittlement, or ballooning; diversity in phase change and interfacial convection during molten core relocation; gap cooling and CCFL models for debris cooling; grain growth & movement and uranium oxidisation during FP release; pool scrubbing and re-evaporation models in FP behaviour; etc. As for the Accident Management evaluation, following models were developed: RPV external cooling of debris; hydrogen mixing and deflagration; PCV venting; ESF effects models; etc.

Following Items will be developed in phase3 (2001-2002):
ATWS, Low power: Nucleonic;
Shut down: Natural circulation; and

).
[5] Andoh, Y. et. al., Development of Fluid - Structure Interaction Analysis Code in the IMPACT Project, ANS 1988 Winter Mtg.
[6] Ujita, H. et. al., Development of LGA & LBE 2D Parallel Programs, International Journal of Mathematical Physics C (Physics and Computer), Vol.9, No.8, 1203-1220, 1998.
[7] Morii, T. et. al., Basic Models and Verification Study on Fuel Rod Heat-Up and Fission Product Release Analysis Modules in SAMPSON for the IMPACT Project, ICONE7, Tokyo, Japan, April, 1999.
[8] Satoh, N. et. al., Development of Molten Core Relocation Analysis Module MCRA in the Severe Accident Analysis Code SAMPSON, *J. Nucl. Sci. Technol.*, **37** [3], 225-236 (2000).
[9] Ujita, H., Hidaka, M., Susuki, A., Ishida, N.: Development of Debris Coolability Analysis Module in Severe Accident Analysis Code SAMPSON for IMPACT Project, *J. Nucl. Sci. Technol.*, **36** [10], 940-952 (1999).
[10] Vierow, K. et. al., Development of the VESUVIUS Code for Steam Explosion Analysis Part 1: Molten Jet Breakup Mbdeling, The Japan Society of Multiphase Flow, Vol. 12 No. 3, September 1998.
[11] Ujita, H., Nagata, S., Satoh, N., et al.: Simulation Supervisory System to Control Analysis Process for Complex Phenomena Simulation in Parallel Environment, IPSJ (submitted for publication to IPSJ).
[12] Schwarz, M., Hache, G., and von der Hardt, P. (1997) "PHEBUS FP: a severe accident research programme for current and advanced light water reactors, " Nucl. Eng. Des., 187, pp. 47-69.
[13] Toda, S. et al. (1994). "Three-dimensional Natural Convection Heat Transfer Inside a Vertical Cylinder Containing Eccentrically Distributed Internal Heat Source", Proc. 10th International Heat Transfer Conference, pp.251-256.
[14] Fujita, Y., et al. (1990). "Boiling Heat Transfer and Critical Heat Flux in a Confined Narrow Space Effects of Gap Size, Inclination Angle, and Peripheral Conditions at the

Space Edge", Heat Transfer 1990, Vol.2, pp.153-158.
[15] Lorenz, R.A. and Osborne, M.F. (1995). "A Summary of ORNL Fission Product Release Tests with Recommended Release Rates and Diffusion Coefficients", NUREG/CR-6261, ORNL/TM-12801.
[16] Rest, J. and Zawadzki, S.A. (1992). "FASTGRASS:A Mechanistic Model for the Prediction of Xe, I, Cs, Ba, an Sr Release from Nuclear Fuel under Normal and Severe-Accident Condition", NUREG/CR-5840, ANL92/3.
[17] Coryell, E.W. et al., NUREG/CR-6150 (EGG-2720), June, 1995.